

# Transient Phenomena in the Pulse Radiolysis of Retinyl Polyenes. 2. Protonation Kinetics<sup>1</sup>

K. Bobrowski<sup>†</sup> and P. K. Das\*

Contribution from the Radiation Laboratory, University of Notre Dame, Notre Dame, Indiana 46556. Received July 27, 1981

**Abstract:** The results of a study are presented concerning the kinetics of reactions of various retinyl derivatives with hydrogen ions released pulse radiolytically in aerated 2-propanol containing 0.5 M acetone and 0.2 M carbon tetrachloride. For retinal and polyene Schiff bases, their protonated forms absorb at much longer wavelengths than the unprotonated substrates and are monitored by kinetic spectrophotometry. In the cases of retinol and retinyl acetate, the initial H<sup>+</sup> adduct undergoes loss of water and acetic acid, respectively, producing the retinyl carbonium ion ( $\lambda_{\max}$  585 nm), which, in turn, decays with first-order kinetics ( $\tau_{1/2} = 10 \pm 3 \mu\text{s}$ ). The rate constants for protonation are in the range  $1 \times 10^7$ – $4 \times 10^9 \text{ M}^{-1} \text{ s}^{-1}$ . In the cases of polyene Schiff bases, the protonation rate constant increases slightly with increasing polyene chain length and is higher for *11-cis*-retinal Schiff base than for its all-trans counterpart. The absorption spectral maxima of protonated polyene Schiff bases observed in the early stages of protonation in the pulse radiolysis are red-shifted by  $\sim 10 \text{ nm}$  relative to those of the protonated forms obtained by adding dilute hydrochloric acid to Schiff base solutions in 2-propanol. This is explained by the lack of ion pairing in the protonated species seen in the pulse radiolysis.

Transient phenomena involving retinyl polyenes are of interest because these molecules play central roles in a variety of biomolecular processes including some that are photoinitiated. In particular, protonation-deprotonation of retinal Schiff bases (RSB) is intimately associated with the events that take place following the excitation of visual pigments<sup>2-4</sup> and is responsible for the shifting of the absorption maxima of the intermediates from high energy to low energy, and vice versa. First, rhodopsin, the visual pigment responsible for vision in grey, has a broad absorption maximum at  $\sim 500 \text{ nm}$  and contains *11-cis*-retinal as chromophore bound to the protein opsin through a protonated Schiff base linkage with the  $\epsilon$ -amino group of a lysine residue.<sup>5</sup> Upon photoexcitation of squid rhodopsin<sup>6</sup> at room temperature, a short-lived species (hypsochromodopsin) with an absorption maximum at 446 nm is formed in less than 28 ps; this, in turn, changes to bathorhodopsin ( $\lambda_{\max}$  534 nm;  $\tau = 300 \text{ ns}$ ) in  $\sim 50 \text{ ps}$ . The short-wavelength absorption maximum of hypsochromodopsin is attributed to proton dislocation,<sup>4,7</sup> which is believed to occur in the singlet excited state during *cis*  $\rightarrow$  *trans* photoisomerization.

Protonated retinal Schiff bases<sup>2,7-9</sup> (PRSB) are not the only systems that have been widely studied as models for visual pigments. Retinyl carbonium ion,<sup>10</sup> generated chemically<sup>11</sup> in strongly acid solutions at low temperatures as well as by flash photolysis<sup>12</sup> of retinol and retinyl acetate, has been examined with a view to understanding the large bathochromic shifts of visual pigments (relative to PRSB) and to shed light on the involvement of charge transfer (if any) in visual excitation. From an extrapolation based on the effects of solvents and counteranions on absorption maxima of PRSB and its higher homologue, it has been shown that in solvents of low dielectric constant the absorption maxima approach those of the corresponding polyene carbonium ions under conditions where there is no electrostatic interaction between the positively charged nitrogen center and the counteranion.<sup>9</sup>

Pulse radiolysis offers a convenient method of generating micromolar concentrations of hydrogen ions in solution on a nanosecond time scale. Using this technique, we have investigated the kinetics of protonation of a number of retinyl polyenes in their ground states. Although the photophysicochemical properties of the products of protonation are fairly well-known, to our best knowledge there has been no work concerning the kinetics and mechanisms of the protonation reactions. While no claim is being made regarding a direct relevance of this study in the understanding of ultrafast proton dislocation in the excited states of visual pigments, the results of the present study concerning ground

states are expected to be of value as a prerequisite. In addition, knowledge regarding the behavior of retinyl polyenes toward hydrogen ions on a short time scale became necessary in interpreting some of the transient phenomena observed by us in the pulse radiolysis<sup>13</sup> of these systems in various solvents.

The structures of the polyenes under examination are shown in Figure 1.

## Experimental Section

*all-trans*-Retinal (Sigma) was chromatographed on a silica gel column with petroleum ether and 10% methyl *tert*-butyl ether as eluent and then crystallized from *n*-hexane. The polyene Schiff bases were prepared by adding excess of *n*-butylamine (Eastman, freshly distilled) to concentrated solutions of the corresponding polyenals in dry methanol and storing these solutions under argon over molecular sieves (3 Å) at 0 °C for  $\sim 12 \text{ h}$ . The solvent and unreacted *n*-butylamine were removed first

(1) The research described herein was supported by the Office of Basic Energy Sciences of the U.S. Department of Energy. This is Document No. NDRL-2269 from the Notre Dame Radiation Laboratory.

(2) Honig, B.; Ebrey, T. G. *Annu. Rev. Biophys. Bioeng.* **1974**, *3*, 151-177.

(3) For an overview of visual pigments and their models, see the articles in: *Acc. Chem. Res.* **1975**, *8*, 81-112.

(4) Shichida, Y.; Kobayashi, T.; Ohtani, H.; Yoshizawa, T.; Nagakura, S. *Photochem. Photobiol.* **1978**, *27*, 335-341.

(5) Collins, F. D. *Nature (London)* **1953**, *171*, 469-471. Morton, R. A.; Pitt, G. A. *J. Biochem. J.* **1955**, *59*, 128-134. Bounds, D. *Nature (London)* **1967**, *216*, 1178-1181. Akhtar, M. P.; Blossie, P. T.; Dewhurst, P. B. *Biochem. J.* **1968**, *110*, 693-702. DeGrip, W. J.; Bonting, S. L.; Daemen, F. J. M. *Biochim. Biophys. Acta* **1973**, *303*, 189-193. Lewis, A. *Spex Industries, Inc.* **1976**, *21*, 1-7.

(6) The  $\lambda_{\max}$  of rhodopsin and the intermediates and the time constants ( $\tau$ ) associated with the formation and decay of the latter depend on the source of rhodopsin and environmental factors. The data quoted here are those for squid rhodopsin in 2% digitonin (pH 10.5 or 7.0) at room temperature (taken from ref 4).

(7) Schaffer, A. M.; Yamaoka, T.; Becker, R. S. *Photochem. Photobiol.* **1975**, *21*, 297-301.

(8) Becker, R. S.; Hug, G.; Das, P. K.; Schaffer, A. M.; Takemura, T.; Yamamoto, N.; Waddell, W. J. *Phys. Chem.* **1975**, *80*, 2265-2273 and references therein.

(9) Blatz, P. E.; Pippert, D. L.; Balasubramanian, V. *Photochem. Photobiol.* **1968**, *8*, 309-315. Blatz, P. E. *Ibid.* **1972**, *15*, 1-6. Blaz, P. E.; Mohler, J. H.; Navangul, H. V. *Biochemistry* **1972**, *11*, 848-855. Blatz, P. E.; Mohler, J. H. *Ibid.* **1972**, *11*, 3240-3242.

(10) Blatz, P. E. *J. Gen. Physiol.* **1965**, *48*, 753.

(11) Blatz, P. E.; Pippert, D. L. *Tetrahedron Lett.* **1966**, 1117-1122; *J. Am. Chem. Soc.* **1968**, *90*, 1296-1300.

(12) Rosenfeld, T.; Alchalal, A.; Ottolenghi, M. *Chem. Phys. Lett.* **1973**, *20*, 291-297. Rosenfeld, T.; Alchalal, A.; Ottolenghi, M. In "Excited States of Biological Molecules"; Birks, J. B., Ed.; Wiley: London, 1976; pp 540-554.

(13) Raghavan, N. V.; Das, P. K.; Bobrowski, K. *J. Am. Chem. Soc.* **1981**, *103*, 4569-4573 (paper I of this series).

<sup>†</sup> On leave of absence from the Institute of Nuclear Research, 03-195 Warsaw, Poland.

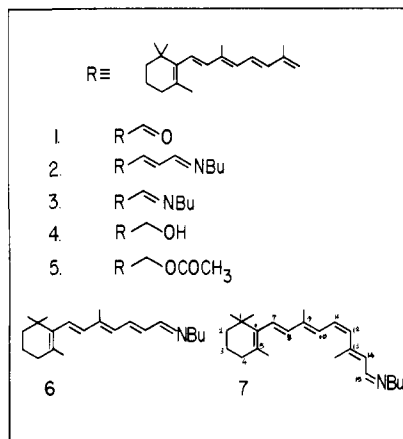


**Figure 1.** Structures of retinyl polyenes under study (all all-trans, except 11-*cis*-retinal Schiff base): (1) retinal; (2) C<sub>22</sub>-*n*-butyl Schiff base (C<sub>22</sub>SB); (3) retinal *n*-butyl Schiff base (RSB); (4) retinol; (5) retinyl acetate (RA); (6) C<sub>17</sub>-*n*-butyl Schiff base (C<sub>17</sub>SB); (7) 11-*cis*-RSB.

by blowing argon over the solutions and then by applying  $\sim 10^{-4}$  torr vacuum. To get rid of the last traces of *n*-butylamine, we repeated 3 times a procedure of dissolving the Schiff base residues in a small quantity of methyl *tert*-butyl ether followed by removal of the solvent (by blowing argon and applying vacuum). This was important because *n*-butylamine, if present, would compete in the protonation reactions of the Schiff bases. For use in preparing the Schiff bases, C<sub>17</sub> and C<sub>22</sub> aldehydes were synthesized and purified by methods described in an earlier paper,<sup>14</sup> and 11-*cis*-retinal was obtained as a gift from Hoffmann-La Roche. Retinyl acetate and retinol, both from Sigma, were used from freshly opened vials without further purification.

2-Propanol (Baker Analyzed or Fisher Spectranalyzed) and carbon tetrachloride (Fisher Spectranalyzed) were used as received. Acetone (Fisher Spectranalyzed) was refluxed over KMnO<sub>4</sub> and then distilled by using a fractionating column. Triethylamine (Eastman) was distilled under vacuum.

A description of the computer-controlled optical pulse radiolysis setup is given elsewhere.<sup>15</sup> Electron pulses (5 ns) from the Notre Dame 7 MeV ARCO LP-7 linear accelerator were used with dose rates of  $\sim 2 \times 10^{16}$  eV/g per pulse. The change in absorbance ( $\Delta OD$ ) following electron irradiation was followed as a function of time by kinetic spectrophotometry and expressed in terms of an extinction coefficient parameter ( $\epsilon'$ ) given by the relationship  $\epsilon' = (\Delta OD \times K)/(G \times \text{dose})$ , where  $K$  is a multiplying factor so chosen that  $\epsilon'$  for (SCN)<sub>2</sub><sup>-</sup> in the same cell is 7600 M<sup>-1</sup>/cm<sup>-1</sup> at 475 nm in N<sub>2</sub>O-saturated aqueous solutions, and  $G$  is the yield per 100 eV.

All pulse radiolysis experiments were carried out in a flow system where the solutions were siphoned from a reservoir through the cell at the rate of  $\sim 15$  mL/min. The rapid flowing of the solutions as well as allowing sufficient time (30–60 s) between shots was important to avoid accumulation of protonation products and to obtain reproducible kinetics and yields. Suitable cutoff filters (Corning) were used to minimize the absorption of the monitoring light by the polyene substrates.

The absorption spectra were measured with a Cary 219 spectrophotometer.

## Results

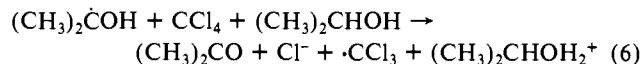
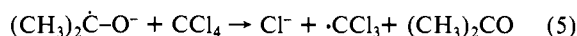
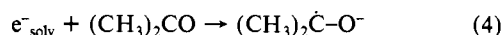
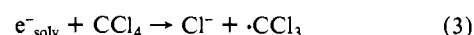
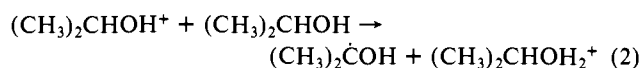
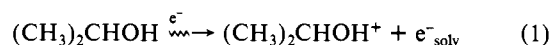
All pulse radiolysis experiments were carried out with air-saturated solutions of the polyene substrates in 2-propanol containing 0.5 M acetone and 0.2 M carbon tetrachloride. In this solvent combination, the initial products of radiolysis, viz., sol-

**Table I.** Protonation Rate Constants and Absorption Maxima of Observed Protonation Products of Various Polyene Substrates in 2-Propanol Containing 0.2 M CCl<sub>4</sub> and 0.5 M Acetone

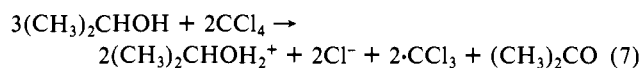
substrate	protonation rate constant, M <sup>-1</sup> s <sup>-1</sup> <sup>a</sup>	$\lambda_{\text{max}}$ , nm <sup>b</sup>
C <sub>17</sub> -SB	$1.7 \times 10^9$	410 (400)
<i>all-trans</i> -RSB	$2.1 \times 10^9$	450 (442)
C <sub>22</sub> -SB	$3.2 \times 10^9$	475 (465)
11- <i>cis</i> -RSB	$3.9 \times 10^9$	450 (441)
TEA	$7.3 \times 10^8$	
retinyl acetate	$2.7 \times 10^7$ <sup>c</sup>	585 (594)
retinol	$2.2 \times 10^7$ <sup>c</sup>	585
retinal	$9.6 \times 10^6$	475

<sup>a</sup> Estimated error  $\pm 15\%$ . <sup>b</sup> The wavelengths in parentheses are the absorption maxima of protonated species obtained by adding dilute hydrochloric acid in 2-propanol, except in the case of retinyl acetate, where 594 nm is the wavelength maximum of retinyl carbonium ion observed in 2-propanol + 58.7 mol % H<sub>2</sub>SO<sub>4</sub> at  $-45^\circ\text{C}$ . <sup>c</sup> These values correspond to the lower limits of the actual protonation rate constants,  $k_{12}$  (see text).

vent-derived cation and solvated electron, undergo reactions as follows:



The net result of steps 1–6 is the production of hydrochloric acid through oxidation of 2-propanol, as summarized in eq 7. Reaction



2 occurs in the spur.<sup>16f,g</sup> Rate constants for reactions 3–6 are available in the literature<sup>16</sup> and are in the range  $1 \times 10^8$ – $2 \times 10^{10}$  M<sup>-1</sup> s<sup>-1</sup>. This means that in the presence of 0.2 M CCl<sub>4</sub> and 0.5 M acetone, steps 2–6 are essentially complete within a short time ( $< 300$  ns)<sup>17</sup> after the electron pulse. The only serious complication that one would anticipate is a chain process initiated by  $\cdot\text{CCl}_3$  through generation of (CH<sub>3</sub>)<sub>2</sub> $\dot{\text{C}}\text{OH}$  by hydrogen abstraction from 2-propanol; however, this is presumably suppressed by the presence of oxygen in the air-saturated solutions we have used. Some experiments were carried with *all-trans*-RSB and retinyl acetate in oxygen-saturated solutions. There was practically no difference in the rates of protonation on replacing air by oxygen; this suggests that chain processes, if any, were of no consequence in the kinetics we have studied at the microsecond time scale.

Another possible source of complication lies in the reactions of retinyl substrates with radicals such as H $\cdot$ , (CH<sub>3</sub>)<sub>2</sub>CHO $\cdot$ , and  $\cdot\text{CCl}_3$  in the form of their addition to polyene chain or hydrogen abstraction by them from methyl groups. Such reactions possibly do occur; however, the radical-type products of these reactions are expected to absorb at shorter wavelengths than the products of protonation we have monitored. For example, the ketyl radical<sup>18</sup>

(14) Das, P. K.; Becker, R. S. *J. Phys. Chem.* **1978**, *82*, 2081–2093.

(15) Patterson, L. K.; Lillie, J. *Int. J. Radiat. Phys. Chem.* **1974**, *6*, 129–141. Schuler, R. H.; Buzzard, G. K. *Ibid.* **1976**, *8*, 563–574.

(16) (a) Köster, R.; Asmus, K. D. *Z. Naturforsch.* **1971**, *26b*, 1104–1108. (b) Radlowski, C.; Sherman, W. V. *J. Phys. Chem.* **1970**, *74*, 3043–3047. (c) Sherman, W. V. *J. Phys. Chem.* **1967**, *71*, 1695–1702. (d) Wilson, R. L.; Slater, T. F. In "Fast Processes in Radiation Chemistry and Biology"; Adams, G. E., Fielden, E. M., Michael, B. D., Eds.; Wiley: New York, 1975; pp 147–161. (e) Sherman, W. V. *J. Phys. Chem.* **1966**, *70*, 667–672. (f) Russell, J. C.; Freeman, G. R. *Ibid.* **1968**, *72*, 808–815. (g) Jha, K. N.; Freeman, G. R. *J. Chem. Phys.* **1969**, *51*, 2846–2850.

(17) The slowest of steps 1–6 is reaction 6 for which the reported rate constant ( $k_6$ ) in water ranges from  $1 \times 10^8$  M<sup>-1</sup> s<sup>-1</sup><sup>16a</sup> to  $7 \times 10^8$  M<sup>-1</sup> s<sup>-1</sup><sup>16d</sup>. Using the lower value of  $1 \times 10^8$  M<sup>-1</sup> s<sup>-1</sup> and allowing for a  $\sim 2$ -fold decrease on going from water to 2-propanol (owing to higher viscosity of the latter), we obtain ca.  $1 \times 10^7$  s<sup>-1</sup> for the slowest step for the release of hydrogen ions under the condition of our experiment. This is more than 6 times faster than the fastest protonation rate we have measured. We think the actual situation is much better because of the presence of oxygen which competes with reactions 2–4 and 6, making them faster, and because  $k_6$  is probably closer to  $7 \times 10^8$  M<sup>-1</sup> s<sup>-1</sup> than to  $1 \times 10^8$  M<sup>-1</sup> s<sup>-1</sup> (in water).

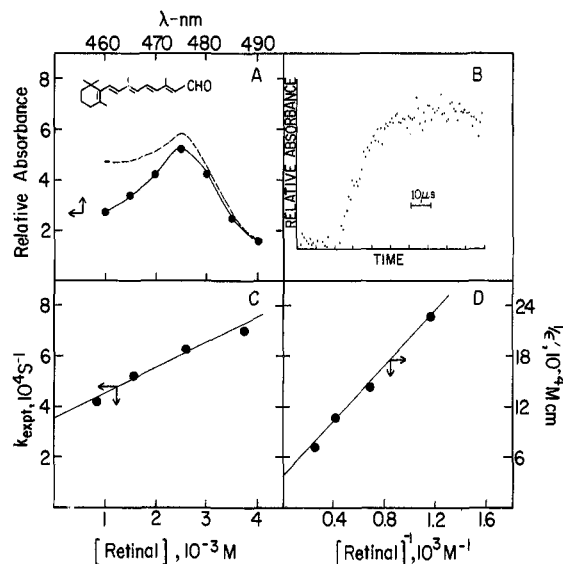
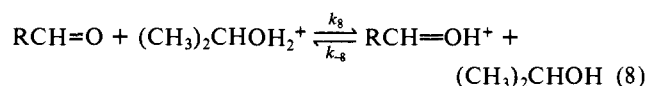


**Figure 2.** (A) Absorption spectrum of protonated form of *all-trans*-retinal ( $8.6 \times 10^{-4}$  M) in 2-propanol containing 0.5 M acetone and 0.2 M  $\text{CCl}_4$  recorded at  $60 \mu\text{s}$  following electron pulse (the dotted curve is obtained after correction for absorption by retinal). (B) Experimental trace showing the formation of protonated retinal at  $\lambda$  475 nm (solution as in A). (C) Plot of the experimental rate constant ( $k_{\text{expt}}$ ) against retinal concentration. (D) Plot of the reciprocal of the relative absorbance observed at  $\lambda$  475 nm against reciprocal of retinal concentration.

of *all-trans*-retinal, that is,  $\text{RCHOH}$ , has been shown to have an absorption maximum at 390 nm in methanol with practically no absorption in the spectral region 410–500 nm. The product(s) of radical addition to retinal (or RSB) or hydrogen abstraction would have electronic configurations similar to that of the retinyl ketyl radical and, therefore, would contribute very little to the absorption assigned as due to the protonation products.

The data concerning rate constants of protonation and absorption spectral maxima of protonated forms (or subsequent products) are given in Table I. The rest of this section is divided according to the nature of the polyenes and the treatment of kinetic data for them.

**(a) *all-trans*-Retinal.** Pulse radiolysis of *all-trans*-retinal ( $(1-4) \times 10^{-3}$  M) in 2-propanol containing 0.2 M  $\text{CCl}_4$  and 0.5 M acetone results in the formation of a species with spectral absorption in the region 450–500 nm ( $\lambda_{\text{max}} \sim 475$  nm). The spectrum and a typical experimental trace for formation are shown in Figure 2A and B, respectively. It is noted that the absorbance corresponding to the plateau region (Figure 2B) is very weak; Figure 2B represents an average of 50 shots. It increases slowly with increasing concentrations of retinal. However, at relatively high concentrations of retinal ( $> 4 \times 10^{-3}$  M), the spectral region 450–500 nm becomes inaccessible because of absorption of the monitoring light by the compound itself. The formation profiles at various concentrations fit well into a first-order growth equation:  $A = A_{\infty}[1 - \exp(-k_{\text{expt}}t)]$  where  $A$  is the absorbance at time  $t$  and  $A_{\infty}$  is the same at plateau. The experimental rate constant,  $k_{\text{expt}}$ , is linearly dependent on retinal concentration, as shown in Figure 2C. We explain these results by assigning the species with  $\lambda_{\text{max}}$  at 475 nm as the protonated form of retinal formed according to 8. Evidence in support of the above assignment is obtained from



the spectral changes observed when dilute hydrochloric acid (0.01–0.001 M) is added to a solution of retinal in ethanol. A prominent tail absorption develops on the long-wavelength side (440–520 nm) of the absorption spectrum of retinal with con-

comitant decrease in the intensity at the maximum (380 nm) of retinal. The isosbestic point is at 420 nm. A quantitative measurement based on addition of larger quantities of hydrochloric acid was not successful because of instability of retinal in highly acidic medium.

A kinetic treatment of the equilibration process represented by eq 8 leads to the following results:

$$k_{\text{expt}} = k_{-8} + k_8[\text{retinal}] \quad (9a)$$

$$A_{\text{eq}}^{-1} = A_{\infty}^{-1} = A_0^{-1}(1 + K^{-1}[\text{retinal}]^{-1}) \quad (9b)$$

$$K = k_8/k_{-8} \quad (9c)$$

where  $k_{\text{expt}}$ , as defined before, is the experimental first-order rate constant for the formation of protonated retinal,  $A_{\text{eq}}$  is the plateau absorbance owing to the protonated retinal after attainment of equilibrium, i.e., at time infinity, and  $A_0$  is the absorbance corresponding to a concentration equal to that of hydrogen ion originally released in the pulse radiolysis.

The utility of eq 9a and 9b is obvious. These offer methods of measurement of not only  $k_8$ ,  $k_{-8}$ , and  $K$  (the equilibrium constant) but also  $A_0$ , which in turn makes it possible to determine the extinction coefficient of the protonated species provided the yield of hydrogen ion,  $G(\text{H}^+)$ , is known. Figure 2, C and D, shows plots based on eq 9a and 9b, respectively. From the slope and the intercept of the linear plot in Figure 2C, we obtain  $k_8 = 9.6 \times 10^6 \text{ M}^{-1} \text{ s}^{-1}$  and  $k_{-8} = 3.5 \times 10^4 \text{ s}^{-1}$ , and hence  $K = k_8/k_{-8} = 270 \text{ M}^{-1}$ . The intercept-to-slope ratio from the plot in Figure 2D gives  $K = 230 \text{ M}^{-1}$ . Considering the errors in the measurement of absorbances and rate constants based on very weak signals, we think the agreement in the values of  $K$  obtained by the two methods is very good. Unfortunately, we could not obtain data over a wider range of concentrations because at higher concentrations, as mentioned earlier, retinal itself absorbs strongly in the region where the protonated species absorbs, rendering its monitoring impossible, and at lower concentrations the signal is too weak to be meaningful.

From the intercept of the linear plot in Figure 2D and by using a  $G$  value of 3.1 for hydrogen ion (measured from protonation of RSB, see later), we obtain an extinction coefficient ( $\epsilon$ ) of  $8000 \text{ M}^{-1} \text{ cm}^{-1}$  at 475 nm for protonated retinal. It should be noted that the error in this number may be as large as  $\pm 50\%$  because of uncertainty in measuring the intercept and use of data based on weak signals. Nevertheless, the small value of the extinction coefficient (relative to retinal) suggests that the spectral region 450–500 nm probably corresponds to a shoulder of the protonated species rather than its absorption maximum. No further transient phenomena were observed at longer wavelengths (500–700 nm) in the concentration range of retinal used,  $(1-4) \times 10^{-3}$  M.

**(b) Polyene Schiff Bases.** In contrast to the case of retinal, pulse radiolysis of polyene Schiff bases (SB) gives rise to very large absorbance changes in the spectral region where their protonated forms absorb. This is understandable when one considers the high extinction coefficients of the protonated Schiff bases in the regions where the unprotonated forms absorb very little and the fact that the equilibrium constants<sup>19</sup> of protonation are so large that the reaction, represented by 10, may be considered irreversible (i.e.,



$k_{-10} \ll k_{10}$ ; see later). To make the absorbance changes smaller and hence reliable and reproducible, we had to select a base, nonabsorbing in both protonated and unprotonated forms at 400–500 nm, to scavenge the hydrogen ions in competition with the reactions with SB's. Triethylamine (TEA) served this purpose very well. In the presence of TEA the first-order rate constant ( $k_{\text{expt}}$ ) for the formation of protonated SB's is given by

$$k_{\text{expt}} = k_0 + k_{\text{T}}[\text{TEA}] + k_{10}[\text{SB}] \quad (11)$$

(19) The measured  $\text{pK}_a$  values<sup>20</sup> of *all-trans*-PRSB are 6.95 in 1:1 water-methanol at  $0^\circ\text{C}$  and 6.23 in water  $0^\circ\text{C}$ .

(20) Blatz, P. E.; Johnson, R. H.; Mohler, J. H.; Al-Dilaimi, S. K.; Dewhurst, S.; Erickson, J. O. *Photochem. Photobiol.* **1971**, *13*, 237–245.

(18) Land, E. J.; Lafferty, J.; Sinclair, R. S.; Truscott, T. G. *J. Chem. Soc., Faraday Trans. 2* **1978**, *74*, 538–545.

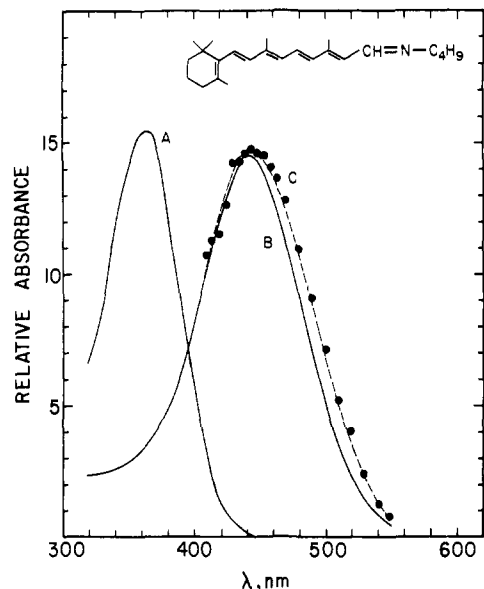


**Figure 3.** (A) Ground-state absorption spectrum of *all-trans*-retinal-*n*-butyl Schiff base (nRSB) in 2-propanol. (B) Absorption spectrum of protonated form of *all-trans*-RSB in 2-propanol produced chemically by adding dilute hydrochloric acid. (C) Absorption spectrum of protonated form of *all-trans*-rSB obtained by pulse radiolysis after the completion of initial protonation process (corrected for the absorption by RSB at 410–450 nm).

where  $k_T$  is the bimolecular rate constant for the protonation of TEA and  $k_0$  includes rate constants such as those related with the reverse of protonation of SB (i.e.,  $k_{-10}$ ) and TEA and with competing, scavenging processes for hydrogen ion by bases generated in the course of pulse of radiolysis (e.g.,  $O_2^-$ ).

Since the spectra of the protonated polyene SB's are available in the literature<sup>9,21</sup> or can be recorded easily by acidification in the solvent we have used, it was a trivial matter to establish the identity of the species seen in pulse radiolysis as the protonated forms. Figure 3 shows a comparison between the spectrum (b) of *all-trans*-PRSB produced chemically by acidifying an *all-trans*-RSB solution in 2-propanol with hydrochloric acid and the spectrum (C) obtained after completion of protonation following the electron pulse. Except for the slight red shift of the species observed in pulse radiolysis, the agreement of the two spectra in shape and location is quite good. Interestingly, the bathochromic shift of the pulse radiolytically generated PRSB, though small ( $\sim 10$  nm), is beyond experimental errors and is also observed in the cases of other polyene Schiff bases. Table I presents the data concerning the spectral maxima of protonated polyene SB's in 2-propanol obtained under the two conditions.

Figure 4 presents two representative plots based on 11; the inset is a typical time profile obtained in a one-shot experiment and used to extract  $k_{\text{exptl}}$ . For the linear plot 4A, [TEA] was kept constant while *all-trans*-RSB concentration was varied; the situation was reversed for the plot 4B. The slope in the former case gives  $k_{10}$  while that in the latter case gives  $k_T$ . It is noted that the intercepts in the two plots 4A and 4B correspond to  $k_0 + k_T[\text{TEA}]$  and  $k_0 + k_{10}[\text{RSB}]$ , respectively; in practice, we found that the measured intercepts in both cases were slightly lower than  $k_T[\text{TEA}]$  (for A) and  $k_{10}[\text{RSB}]$  (for B), calculated using known values of the rate constants and concentrations. Within the uncertainty in the determination of the intercepts, this result is taken to mean that  $k_0$  in eq 11 is small and negligible.

Protonation studies with polyene SB's permit us to make an estimate of the yield,  $G(\text{H}^+)$ , of hydrogen ions produced under the conditions of our experiments. An assumption necessary for this purpose is that the maximum extinction coefficients ( $\epsilon_{\text{max}}$ 's) of the protonated polyene SB's observed in the pulse radiolysis

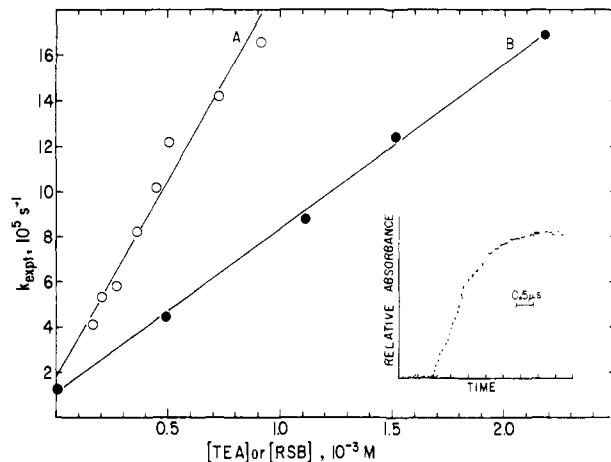
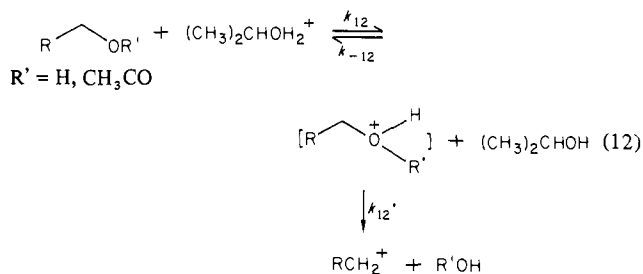


**Figure 4.** Plots of  $k_{\text{exptl}}$  against concentration of (A) *all-trans*-RSB in the presence of  $4.4 \times 10^{-4}$  M TEA and of (B) TEA in the presence of  $9.2 \times 10^{-5}$  M *all-trans*-RSB. Inset: Experimental trace at  $\lambda$  450 nm showing the formation of *all-trans* protonated RSB in a solution containing  $4.4 \times 10^{-4}$  M TEA and  $4.5 \times 10^{-4}$  M *all-trans*-RSB.

are equal to  $\epsilon_{\text{max}}$ 's of those produced chemically by adding dilute hydrochloric acid to SB solutions in 2-propanol. From experiments done with *all-trans*-RSB solutions in the concentration range  $(2-5) \times 10^{-3}$  M in the presence of  $4.4 \times 10^{-4}$  M TEA and after proper correction of PRSB yield for the partitioning of the consumption of hydrogen ions between TEA and RSB, we obtained  $3.1 \pm 0.3$  for  $G(\text{H}^+)$ .

(c) *all-trans*-Retinol and Retinyl Acetate. Protonation of *all-trans*-retinol and its acetate ester leads to the formation of retinyl carbonium ion through the loss of water or acetic acid from the initially formed  $\text{H}^+$  adduct. The steps in the reaction are as follows:



The spectra of  $\text{RCH}_2^+$ , shown in Figure 5, have maxima at 585 nm in the cases of both retinol and retinyl acetate as substrate and are similar to those obtained chemically<sup>11</sup> by adding a strong acid at low temperature as well as by flash-photolytic dissociation.<sup>12</sup> The species  $\text{RCH}_2^+$  is observed in measurable yields only at relatively high concentrations ( $>10^{-3}$  M) of the substrates. At these high concentrations, no attempt to observe the  $\text{H}^+$  adduct  $\text{RCH}_2\text{OHR}'^+$ , i.e., the precursor of  $\text{RCH}_2^+$ , could be made because the spectral region 350–450 nm was not accessible owing to absorption of the monitoring light by the substrates. Even in dilute solutions ( $10^{-5}$ – $10^{-4}$  M), no significant spectral absorption attributable to that by  $\text{RCH}_2\text{OHR}'^+$  could be detected beyond the tailing of the ground-state absorption. This can be explained by the fact(s) that the spectra of  $\text{RCH}_2\text{OHR}'^+$  and  $\text{RCH}_2\text{OR}'$  probably do not differ significantly and/or that the rate of the conversion of  $\text{RCH}_2\text{OHR}'^+$ s into  $\text{RCH}_2^+$  (determined by  $k'_{12}$ ) is much faster than that of its formation (determined by  $k_{-12} + k_{12}[\text{RCH}_2\text{OR}']$ ) in dilute solutions.

As implied by eq 12 the formation kinetics of  $\text{RCH}_2^+$  would be a complex one, particularly under conditions where  $k_{12}$ – $[\text{RCH}_2\text{OR}']$ ,  $k_{12}$ , and  $k'_{12}$  are comparable. This situation is further complicated by the fact that in dilute solutions, the decay rate of  $\text{RCH}_2^+$  (see later) becomes nonnegligible in comparison to their formation rates and a clearly defined, flat plateau is not obtained in the growth profiles. However, at relatively high concentrations

(21) Das, P. K.; Kogan, G.; Becker, R. S. *Photochem. Photobiol.* **1979**, *30*, 689–695.

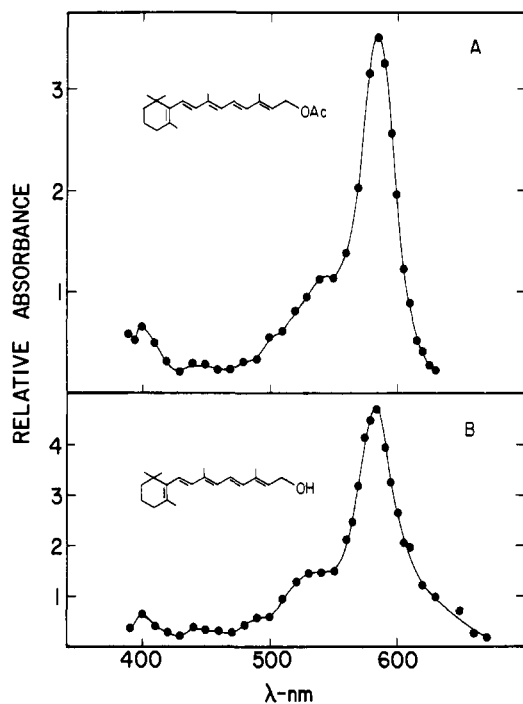


**Figure 5.** Absorption spectra of retinyl carbonium ion (A) in  $1.2 \times 10^{-3}$  M retinyl acetate solution observed at  $13 \mu\text{s}$  after the pulse and in (B)  $2.5 \times 10^{-3}$  M retinol solution observed at  $6.4 \mu\text{s}$  after the pulse.

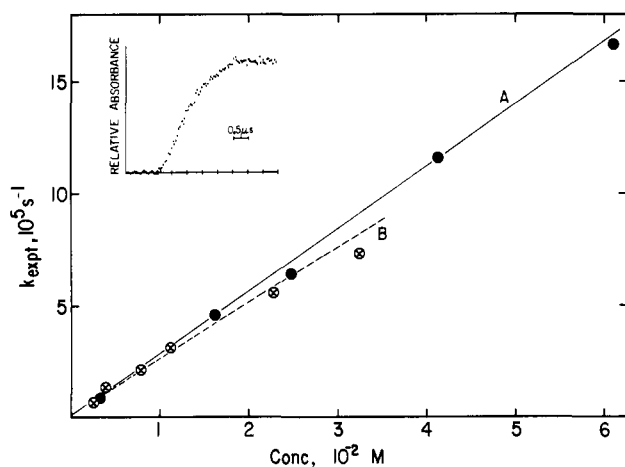


**Figure 6.** Plots of  $k_{\text{exptl}}$  for formation of  $\text{RCH}_2^+$  against concentration of (A) retinyl acetate and (B) retinol, according to eq 13. Inset: Experimental trace at  $\lambda$  585 nm showing the formation of  $\text{RCH}_2^+$  in  $4.1 \times 10^{-2}$  M retinyl acetate solution.

(20–60 mM) the decay of  $\text{RCH}_2^+$  was negligible during the time in which its formation was complete. Under these conditions, the experimental traces for  $\text{RCH}_2^+$  formation could be fitted acceptably into a single exponential, integrated growth equation.<sup>22</sup> It can be shown that under such conditions, the experimental rate constant  $k_{\text{exptl}}$  for formation of  $\text{RCH}_2^+$  is given by<sup>23</sup>

$$k_{\text{exptl}} = \left( \frac{k'_{12}}{k'_{12} + k_{-12}} \right) k_{12} [\text{RCH}_2\text{OR}'] \quad (13)$$

(22) Some experiments were done to observe the formation of *all-trans*-PRSB (at 450–500 nm) in competition with the reaction of hydrogen ion with retinyl acetate in solutions containing both substrates. The observed growths of PRSB under these conditions were found to be of first order, and the corresponding rate constants increased linearly with retinyl acetate concentrations.

(23) The situation is similar to the quenching of an excited-state species (e.g., carbonyl triplet) through reversible exciplex formation followed by the decay of the exciplex and/or photoproduct formation from it. A kinetic analysis of such a scheme is available: Fang, T.-S.; Brown, R. E.; Kwan, C. L.; Singer, L. A. *J. Phys. Chem.* **1978**, *82*, 2489–2496.

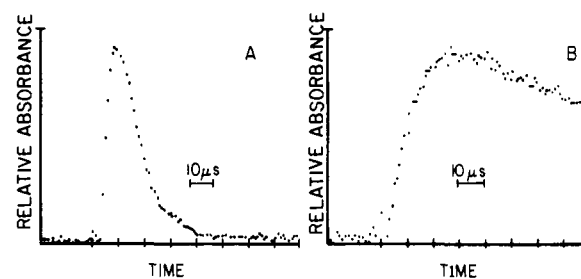
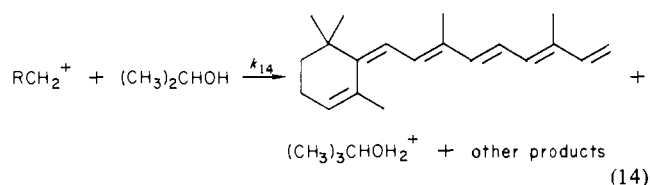


**Figure 7.** Experimental traces in  $2 \times 10^{-3}$  M retinol solution corresponding to (A) decay of retinyl carbonium ion at  $\lambda$  585 nm and (B) simultaneous formation of long-lived species (see explanation in text) at  $\lambda$  410 nm.

provided  $k_{12}[\text{RCH}_2\text{OR}']$  is small compared to  $k'_{12}$ . Figure 6 shows the plots of  $k_{\text{exptl}}$  vs. substrate concentration, based on eq 13. As expected, the plots are reasonably linear and have intercepts close to zero.

The fate of the carbonium ion  $\text{RCH}_2^+$  is of interest. Its decay is found to follow a clean, first-order kinetic behavior. The observed lifetime for decay, obtained as the average of five measured values in the concentration range  $10^{-3}$ – $10^{-2}$  M (for retinyl acetate), is  $14 \pm 4 \mu\text{s}$ ; this is practically unaffected by the presence of larger concentrations of oxygen (e.g., in oxygen-saturated solutions). The first-order decay behavior of  $\text{RCH}_2^+$  can be explained in terms of loss of a proton forming polyene(s) with six double bonds (eq 14). As a matter of fact, anhydrovitamin A, shown in eq 14, has



been synthesized<sup>24</sup> via protonation of retinol. Figure 7A shows an experimental trace corresponding to complete decay of  $\text{RCH}_2^+$  (at 585 nm). Since anhydrovitamin A absorbs strongly in the spectral region 350–420 nm,<sup>24</sup> it should, in principle, be possible to observe its formation at short wavelengths at the same time scale as that of the decay of  $\text{RCH}_2^+$ . Figure 7B shows a trace at 410 nm, where, in fact, formation of long-lived species is observed. However, as evident from Figure 7B, there is a tendency of the product(s) to decay on a longer time scale, suggesting that there are contributions from additional processes, probably involving radical-type species.

The quenching behavior of the carbonium ion  $\text{RCH}_2^+$  toward TEA and  $\text{Br}^-$  (added as tetrabutylammonium bromide) has been studied with generation of this species from both retinol and retinyl acetate. The quenching behavior, as expected, was practically immaterial of whether retinol or retinyl acetate was used as the starting substrate. With TEA, the quenching of  $\text{RCH}_2^+$  may arise because of the formation of tetraalkylammonium cation species,  $(\text{RCH}_2)\text{N}(\text{C}_2\text{H}_5)_3^+$ , with the polyene being attached to nitrogen via  $\text{C}_5$  or  $\text{C}_{15}$  and/or through participation of TEA as a base in the deprotonation process (similar to eq 14, where 2-propanol is replaced by TEA). With increasing TEA concentrations, in addition to the decay of  $\text{RCH}_2^+$  becoming faster, we observe a gradual decrease in the yield of  $\text{RCH}_2^+$  as well as an increase in its formation rate. This is readily understandable in terms of the role of TEA as a quencher not only for  $\text{RCH}_2^+$  but also for hydrogen ions (in competition with  $\text{RCH}_2\text{OR}'$ ). From plots based on  $k_d = k_{14} + k_q[\text{Q}]$  where  $k_d$  is the experimental first-order decay rate constant at quencher (i.e., TEA or  $\text{Br}^-$ ) concentration  $[\text{Q}]$  and  $k_q$  is the bimolecular quenching rate constant, we obtain  $(1.6 \pm 0.2) \times 10^6$  and  $1.9 \pm 0.4 \times 10^9$  for TEA and  $\text{Br}^-$ ,<sup>25</sup> respectively.

(24) Christensen, R. L.; Kohler, B. E. *Photochem. Photobiol.* **1973**, *18*, 293–301. Shantz, E. M.; Cawley, J. D.; Embree, N. D. *J. Am. Chem. Soc.* **1943**, *65*, 901–906. Auerbach, R. A.; Granville, A. M. F.; Kohler, B. E. *Biophys. J.* **1979**, *25*, 443–454.

The extinction coefficient ( $\epsilon_{\max}$ ) of  $\text{RCH}_2^+$  has been estimated from the absorbance at 585 nm in the limit of high concentration of the substrates. On the basis of  $G(\text{H}^+) = 3.1$ ,  $\epsilon_{\max}$  is found to be  $40\,000 \pm 5\,000 \text{ M}^{-1} \text{ cm}^{-1}$ . This value agrees very well with that reported<sup>11</sup> for methanol + 51.1 mol %  $\text{H}_2\text{SO}_4$  at  $-45^\circ\text{C}$  ( $\epsilon_{\max} = 4.4 \times 10^4 \text{ M}^{-1} \text{ cm}^{-1}$  at 589 nm) but is much smaller than that reported<sup>11</sup> for 2-propanol + 58.7 mol %  $\text{H}_2\text{SO}_4$  at  $-45^\circ\text{C}$  ( $\epsilon_{\max} = 6.7 \times 10^4 \text{ M}^{-1} \text{ cm}^{-1}$  at 594 nm).

### Discussion

As exemplified by the present work, the pulse radiolytic release of hydrogen ions combined with kinetic spectrophotometry offers a clean, convenient, and controllable method of studying fast protonation kinetics and of observing the protonation products at the early stage of their formation. This is particularly true when the protonated species or the products derivable from them have absorption spectra separated from those of the starting substrates (e.g., polyene SB's and retinol/retinyl acetate); in other cases (e.g., TEA) where direct spectrophotometric monitoring is not feasible, one can employ competition techniques with the help of a proper acid-base color indicator. There is, of course, the scope of obtaining corroborative kinetic data by measuring conductivity changes.

An explanation is desirable for our observation that the protonated SB's monitored in the pulse radiolysis at the early stage of protonation have absorption spectral maxima red-shifted by  $\sim 10$  nm relative to the maxima of the corresponding protonated species obtained by adding dilute hydrochloric acid to SB solutions in 2-propanol. We think the spectral shift comes from the contribution of ion pairing in the latter case. In other words, the protonated species observed in the pulse radiolysis has, at the initial stage, only the polar solvent molecules in the neighborhood of the positively charged nitrogen center and slowly undergoes pairing with the counterion ( $\text{Cl}^-$ ) to form the species seen in the usual chemical method of preparation (i.e., by adding dilute hydrochloric acid). Regulation of spectral maxima of retinyl and related polyene SB's (protonated) by counteranions through electrostatic interaction is quite well documented.<sup>9</sup> The absorption maximum moves to higher energies as the radius of the anion decreases.

Perhaps the most interesting finding in the present study is the dependence of protonation rate constants of polyene SB's on polyene chainlength and geometry. Considered in the light of the fact that 2-propanol is a relatively viscous solvent, the protonation rate constants ( $k_{10}$ ) of SB's, listed in Table I, are in the vicinity of diffusion control. As the polyene chain length is increased, a slight increasing trend is noticed in  $k_{10}$ . Apparently, this result is not in conformity with the results of a study<sup>26</sup> concerning

charge-transfer interaction (ground state) of polyene SB's with various electron acceptors. On the basis of the experimentally observed trend in the equilibrium constant of charge-transfer complex formation and supported by CNDO/INDO calculations, it has been concluded<sup>26</sup> that the electron-donating ability of a polyene SB, via the nonbonding lone pair of electrons on the N atom, decreases as the chain length becomes longer. Relative to charge transfer, protonation involves a stronger interaction (covalent) at a shorter range. Our result concerning the lack of a pronounced sensitivity of protonation rate with respect to chain length supports the conclusion, based on semiempirical calculations,<sup>26</sup> that  $^+\text{N-H}$  bond order at the ordinary N-H distance of 1 Å in protonated polyene SB's remains practically unchanged on increasing chainlength. Also, between the all-trans and 11-cis isomers of RSB (Table I), the latter reacts with hydrogen ions at a faster rate. This suggests increased basic character in the imino nitrogen of the 11-cis isomer. Dielectric studies<sup>27</sup> with *all-trans*- and 11-*cis*-retinal in methylcyclohexane have shown that the 11-cis isomer has a slightly smaller dipole moment (3.89 D) than the all-*trans* one (4.02 D). Qualitatively similar conclusions have been drawn from the results of an all-valence-electron CNDO/S calculation.<sup>28</sup> Assuming that the isomeric dependence of dipole moment is similar in polyene aldehydes and Schiff bases, one would expect the two RSB isomers to be more or less equally favored substrates for protons. Our results, however, suggest that the geometric dependencies of dipole moment and basicity of imino nitrogen in RSB's are not necessarily parallel.

It is noted that the protonation rate constant for *all-trans*-retinal is smaller than that for *all-trans*-RSB by more than two orders of magnitude. This is not surprising in view of lower basicity of carbonyl oxygen than imino nitrogen. The same trend is also noted for the equilibrium constant for the formation of  $\text{H}^+$  adduct, eq 8 and 9. Interestingly, the observable lowest energy absorption maximum (possibly a prominent shoulder) of protonated retinal,  $\text{RCHOH}^+$ , is similar to that of protonated RSB; this suggests that the contributions of carbonium ion type structures such as  $\text{RCH}^+\text{OH}$  or  $\text{RCH}^+\text{NHBu}$  leading to delocalization of positive charge along the polyene chain are as small in the case of protonated retinal as in the case of protonated RSB.

**Acknowledgment.** We are grateful to Dr. P. Neta for suggesting the proper solvent combination for pulse radiolytic generation of hydrogen ions and for many valuable discussions.

**Registry No.** Retinyl acetate, 127-47-9; retinol, 68-26-8; retinal, 116-31-4; *all-trans*-RSB, 36076-04-7; *all-cis*-RSB, 52647-48-0; TEA, 121-44-8;  $\text{C}_{17}$ -SB, 73432-29-8;  $\text{C}_{22}$ -SB, 73432-32-3.

(25) The plot of  $k_d$  against tetrabutylammonium bromide concentration was slightly bent downward at higher concentrations, understandably because of incomplete ionization of the salt.  $k_d$  was determined from the slope of the plot in the low concentration limit.

(26) Barboy, N.; Feitelson, J. *Photochem. Photobiol.* **1978**, *28*, 421-434.

(27) Bauer, P.-J.; Carl, P. *J. Am. Chem. Soc.* **1977**, *99*, 6850-6855.

(28) Weimann, L. J.; Maggiora, G. M.; Blatz, P. E. *Int. J. Quantum Chem., Quantum Biol. Symp.* **1975**, *2*, 9-24.